Est. 1984

ORIENTAL JOURNAL OF CHEMISTRY
An International Open Access, Peer Reviewed Research Journal

www.orientjchem.org

ISSN: 0970-020 X
CODEN: OJCHEG
2018, Vol. 34, No.(6):
Pg. 2716-2720

Enantiomeric Polylactide Blends in the Presence of Montmorillonite Clay

ONANONG CHEERAROT* and YODTHONG BAIMARK

Biodegradable Polymers Research Unit, Department of Chemistry and Center of Excellence for Innovation in Chemistry, Faculty of Science, Mahasarakham University, Mahasarakham 44150, Thailand.
*Corresponding author E-mail: E-mail: onanong.c@msu.ac.th

http://dx.doi.org/10.13005/ojc/340604

(Received: May 26, 2018; Accepted: December 07, 2018)

ABSTRACT

The stereocomplex polylactides (scPLAs) of the asymmetric poly(L-lactide)(PLLA)/poly (D-lactide) (PDLA) ratios from 80:20 to 60:40 were prepared via the simple melt blending method using an internal mixer at 200^{O}C. An organo-modified clay, Cloisite® 30B, was used for nanocomposite preparation. The formation of the stereocomplex and nanocomposite structures were confirmed by differential scanning calorimetry (DSC), wide-angle X-ray diffraction (WAXD) and transmission electron microscopy (TEM). An increase in the PDLA content could enhance the stereocomplex formation. The presence of Cloisite®30B decreased the melting temperature and crystallinity of the blends. This was due to the thinner crystalline size generated and/or more disordered crystals.

Keyword: Clay, Stereocomplex, Polylactide, Blends, Enantiomer

INTRODUCTION

Polylactide or poly(lactic acid) (PLA) is a biodegradable polyester developed from renewable resources.[1] PLA exists in three typical enantiomer forms, namely poly(L-lactide) (PLLA), poly(D-lactide) (PDLA), and poly(D,L-lactide) (PDLLA), which exhibit widely different properties.[2,3] Because of strong interactions between PLLA and PDLA chains, the blending of PLLA and PDLA leads to the formation of stereocomplex crystallites possessing properties that differ significantly from those of their neat enantiomers.[4,5] The stereocomplex formation enhances the properties of the PLA, including hydrolysis resistance[6], thermal stability[7,8], and mechanical properties. [9,10]

There have recently been several attempts to widen the end-use properties of PLA by formulating stereocomplex-clay nanocomposites formations using 50/50 symmetric PLLA/PDLA ratio.[11-15] However, to the best of our knowledge, there have been no reports investigating asymmetric stereocomplexing of PLLA/PDLA blends containing Montmorillonite clay. Hence, this work addressed stereocomplex formation and thermal stability of the PLLA/PDLA blends in the presence of clay. In the first step, PLLA and PDLA, were synthesized with similar number-average molecular weights. Next, their series of asymmetric blends were prepared. Cloisite® 30B was selected to use due to it being compatible with PLA. Then, the stereocomplex formation and

This is an Open Access article licensed under a Creative Commons license: Attribution 4.0 International (CC- BY).
Published by Oriental Scientific Publishing Company © 2018

nanocomposite structure was characterized using differential scanning calorimetry (DSC), transmission electron microscopy (TEM) and wide-angle X-ray diffraction (WAXD).

EXPERIMENTAL

Materials

PLLA and PDLA were synthesized by ring-opening polymerization under a N_2 atmosphere using stannous octoate as a catalyst and 1-dodecanol as an initiator. More details regarding the synthesis can be found in a previous paper by this group[16]. The number-average molecular weight characteristics and L enantiomer contents of the PLLA and PDLA are presented in Table 1. Cloisite® 30B (designated C30B) was kindly provided by BYK Additives Limited, and produced by the modification of sodium montmorillonite with methyl, tallow, bis-2-hydroxyethyl, quaternary ammonium chloride. The modifier concentration for Closite® 30B was 90 meq/100 g clay.

Table 1: Characteristics of PLLA and PDLA homopolymers

Sample	M_n[a] (g/mol)	MWD	L enantiomer content (%)[b]
PLLA	85,400	2.1	96
PDLA	88,400	2.2	3

[a]Obtained from GPC curves.
[b]Calculated from specific rotation

Sample preparation

Prior to blend preparation, PLLA, PDLA, and Cloisite®30B were vacuum dried at 60°C for 24 hours. Various formulations were prepared via a melt blending technique using an internal mixer (HAAKE Polylab OS system) at 100 rpm, 200°C for 3 minute. For comparative purposes, neat PLLA was prepared using the same operating conditions and was used as a reference. The contents of the clay were fixed at 3 wt% based on total blend weight (Table 2).

Table 2: Formulations of studied blends in wt%

Sample	PLLA	PDLA	C30B
Neat PLLA	100		
80L20D	80	20	
70L30D	70	30	
60L40D	60	40	
80L20D + 3% C30B	77.6	19.4	3
70L30D + 3% C30B	67.9	29.1	3
60L40D + 3% C30B	58.2	38.8	3

Characterization

DSC was performed by a Perkin-Elmer Pyris Diamond under a flow of nitrogen. Samples of 5 mg were accurately weighed and encapsulated in aluminium pans; an empty pan was used as a reference. The samples were heated over a temperature range of 0 to 255°C at 10°C min^{-1} (the 1st heating scan) and then quenched to 0°C using the DSC instrument's own default cooling mode before heating from 0 to 255°C (the 2nd heating scan).

WAXD was performed at 25°C using a Bruker D8 Advance wide-angle X-ray diffractometer using Cu-Kα radiation (λ = 0.15406 nm) using a voltage of 40 kV and a filament current of 40 mA. Data were collected in the θ-2θ mode with a scan speed of 3° min^{-1} in the 2θ scanning range of 2-30°. From the position of a peak, the corresponding d spacing was calculated from the Bragg's diffraction equation:

$$2d \sin\theta = n\lambda \quad (1)$$

For the TEM analysis, specimens were embedded in epoxy resin and taken from a microtome section, which were about 70 nm thick and mounted in a copper grid. A TEM (Philips-Tecnai 20) operated at 120 kV was employed for the observation.

RESULTS AND DISCUSSION

Stereocomplex formation

DSC and WAXD confirmed the formation of the stereocomplex in the melt blends. The 2nd heating scan DSC thermograms of the neat PLA and PLLA/PDLA blends are shown in Fig. 1(a). There was only a melting endothermic peak at 170°C for the neat PLA, whereas the PLLA/PDLA blends displayed double melting endothermic peaks at 170 °C and 230°C. This indicated that two types of crystal appear in the PLLA/PDLA blends. The lower melting peak corresponded to the homo-crystallites and the higher melting peak corresponded to stereocomplex crystallites.[17] Table 3 summarizes the DSC results. As the amount of PDLA in the blend increased, the melting peak area of the homo-crystallites decreased and the stereocomplex increased. It has been suggested that the homo-crystallites were rearranged to the stereocomplex crystallites.[11]

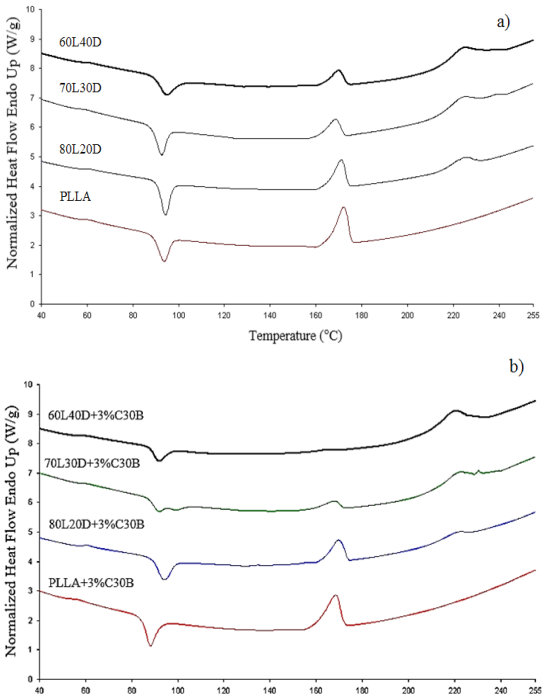

Fig. 1. 2nd heating scan dsc thermograms of (a) asymmetric PLLA/PDLA blends and (b) PLLA/PDLA/clay blends

The DSC thermograms of the PLLA/PDLA blends containing nanoclay are shown in Fig. 1(b). The DSC results are also presented in Table 3. The presence of clay slightly decreased both the $T_{m,hc}$ and $T_{m,sc}$ of the blends. These results were attributed to the smaller crystalline size and/or the presence of imperfect crystals due to polymer-clay interactions.[18,19]

The crystallinity of the PLA homo-crystallites (X_{hc}) was calculated based on equation (2) by assuming a melting enthalpy of 93 J g^{-1} for 100% crystallized PLA, whereas the crystallinity of the PLA stereocomplex crystallites (X_{sc}) was calculated using equation (3) and 142 J g^{-1} was used for the perfect stereocomplexation.[20]

$$X_{hc}(\%) = (\Delta H_{hc}/ (W_{scPLA} \times 93\ J/g) \times 100\% \quad (2)$$

$$X_{sc}\ (\%) = (\Delta H_{sc}/ (W_{scPLA} \times 142\ J/g) \times 100\% \quad (3)$$

Where PLA is the weight fraction of scPLA Table 3 reveals that X_{sc} of the PLLA/PDLA blends significantly increased as the PDLA ratios increased, which suggested an interaction between PLLA and PDLA leading to stereocomplex formation. However, both the X_{hc} and the X_{sc} of the PLLA/PDLA blends significantly decreased as the nanoclay was added for the same PLLA/PDLA blend ratio. These results can be explained by the intercalation of the polymer chains into the clay galleries due to the polymer-clay interaction that may interrupt both the homo- and the stereocomplex crystallization.

Table 3: Thermal transition properties of PLLA/PDLA blends derived from 2nd heating scans dsc thermograms

Samples	$T_{m,hc}$ (°C)	$\Delta H_{m,hc}$ (J g^{-1})	X_{hc} (%)	$T_{m,sc}$ (°C)	$\Delta H_{m,sc}$ (J g^{-1})	X_{sc} (%)
Neat PLLA	172	43.8	47.1	-	-	-
80L20D	171	34.0	36.5	225	15.5	10.9
70L30D	169	20.9	22.4	224	30.7	21.6
60L40D	170	13.2	14.2	224	37.7	26.5
80L20D + 3% C30B	169	28.3	30.4	221	9.7	6.8
70L30D + 3% C30B	167	11.9	12.9	221	26.6	18.7
60L40D + 3% C30B	167	4.9	5.2	221	31.4	22.1

The crystalline structures of the homo-crystallites and stereocomplex crystallites were studied from the WAXD patterns, which are presented in Fig. 2(a). Neat PLA revealed the presence of peaks at 16.5° and 18.1°. However, the WAXD patterns of the PLLA /PDLA blends showed three main diffraction peaks with 2θ values of 12°, 21°, and 24°, which corresponded to the X-ray diffraction peaks of the PLA stereocomplexation reported by Ikada *et al.,*[5] The diffraction peak intensities of the stereocomplex crystallites were enhanced as the amount of PDLA increased. These results indicated that the stereocomplex crystallites were formed in the melt mixture of the PDLA and PLLA during preparation. In addition, the diffraction peaks of the clay-based nanocomposites remained in nearly the same positions as the PLLA/PDLA blends (Fig. 2 b). This indicated that the crystal structure of the PLLA/PDLA blends remained unchanged despite the addition of clay.

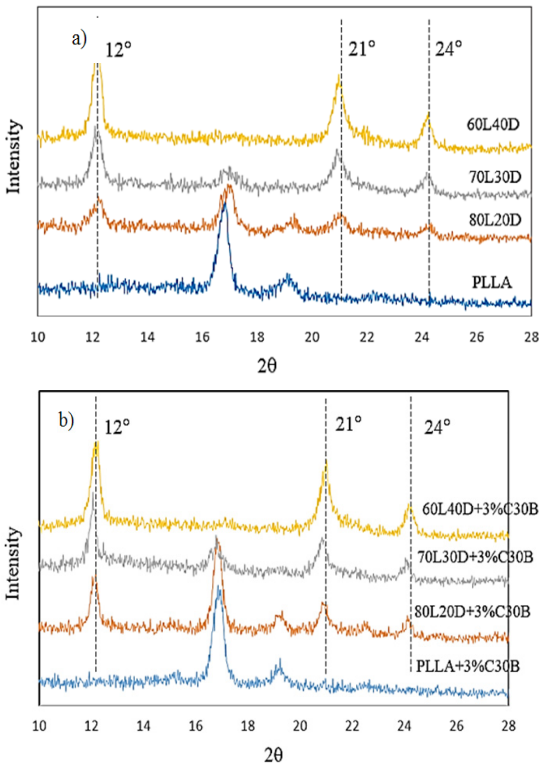

Fig. 2. WAXD profiles of (a) asymmetric PLLA/PDLA blends and (b) PLLA/PDLA/clay blends

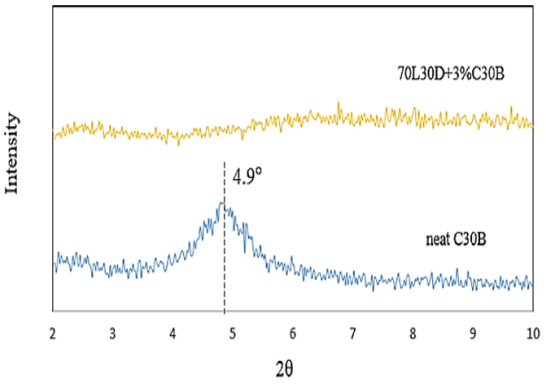

Fig. 3. WAXD profiles of neat c30B and 70L60D in the presence of cloisite® 30B

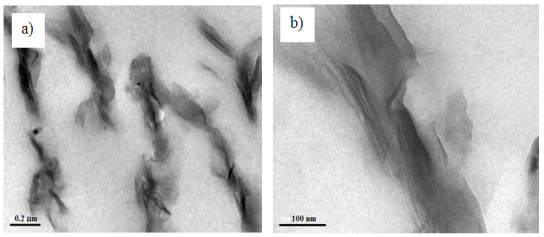

Fig. 4. TEM images of 70L30D in the presence of cloisite® 30B 3wt% at (a) low magnification and (b) high magnification (bar scales = 0.2 μM and 100 nm,

Nanocomposites structures

Besides proving and reconfirming the degree of stereocomplexation, the information provided from the WAXD measurements can be related to the structure of the nanocomposites. As shown in Fig. 3, the pristine C30B shows a diffraction peak at $2\theta = 4.90^{o}$, corresponding to d001 spacing of 1.80 nm. For a nanocomposite of a 70L30D blend with C30B clay, the WAXD pattern did not show a peak between $2<2\theta<10$ corresponding to the basal spacing of C30B due to high layer spacing (more than 6-7 nm) and/or relatively disordered structures.[22] However, information from WAXD alone is insufficient to give definitive conclusions about the defined structure. Thus, TEM was utilized to verify the results of WAXD. Fig. 4 shows the TEM micrographs of the nanocomposites structures at different magnifications. The grey areas represent the stereocomplex PLA matrix, whereas the dark lines correspond to clay sheets. It was observed the clay platelets dispersed and intercalated within the scPLA matrix. These observations are consistent with the WAXD results.

CONCLUSION

The scPLAs of PLLA/PDLA blends with and without Cloisite® 30B nanoclay addition were prepared via a simple melt blending method. An increase in the PDLA content could enhance the stereocomplex formation and thermal stability. The addition of nanoclay significantly decreased the crystallization due to the intercalation of the polymer chains into the clay galleries. Also, there was a decrease in melting temperature of the blends. This was due to the intercalation of polymer-clay by generated the smaller crystalline sized and/or the present of imperfect crystals. The TEM images of the blends showed that the clay platelets were intercalated and dispersed in the blends.

ACKNOWLEDGEMENT

The authors gratefully acknowledge financial supported provided by Mahasarakham University and the National Research Council of Thailand (NRCT). The Center of Excellence for Innovation in Chemistry (PERCH-CIC), Commission on Higher Education, Ministry of Education, Thailand is also acknowledged.

REFERENCES

1. Saeidlou, S.; Huneault, M. A.; Li, H. B.; Park, C. B., *Polymer.*, **2013**, *54*, 5762-5770.
2. Anderson, K. S.; Hillmyer, M. A., *Polymer.*, **2006**, *47*, 2030-2035.
3. Chang, L.; Woo, E. M., *Polymer.*, **2011**, *52*, 68-76.
4. Ahmed, J.; Varshney, S. K.; Janvier, F., *J. Therm. Anal. Calorim.*, **2014**, *115*, 2053-2061.
5. Ikada, Y.; Jamshidi, K.; Tsuji, H.; Hyon, S. H., *Macromolecules.*, **1987**, *20*, 904-906.
6. Tsuji, H., *Polymer.*, **2000**, *41*, 3621-3630.
7. Tsuji, H.; Fukui, I., *Polymer.*, **2003**, *44*, 2891-2896.
8. Brizzolara, D.; Cantow, H. J.; Diederichs, K.; Keller, E.; Domb, A. J., *Macromolecules.*, **1996**, *29*, 191-197.
9. Rathi, S.; Chen, X.; Coughlin, E. B.; Hsu, S. L.; Golub, C. S.; Tzivanis, M. J., *Polymer.*, **2011**, *52*, 4184-4188.
10. Tsuji, H.; Ikada, Y., *Polymer.*, **1999**, *40*, 6699-6708.
11. Furuhashi, Y.; Morioka, K.; Tamegai, H.; Yoshie, N., *J. Appl. Polym. Sci.*, **2013**, *127*, 1615-1622.
12. Purnama, P.; Lim, S. H.; Jung, Y.; Kim, S. H., *Macromol. Res.*, **2012**, *20*, 545-548.
13. Lo Re, G.; Benali, S.; Habibi, Y.; Raquez, J. M.; Dubois, P., *Eur. Polym. J.*, **2014**, *54*, 138-150.
14. Li, Y.; Han, C. Y.; Zhang, X.; Xu, K.; Bian, J. J.; Dong, L. S., *Polym. Eng. Sci.*, **2014**, *54*, 914-924.
15. Purnama, P.; Jung, Y.; Kim, S. H., *Macromol. Mater. Eng.*, **2013**, *298*, 263-269.
16. Baimark, Y.; Srihanam, P., *Polym. Testing.,* **2015**, *45*, 52-57.
17. Tsuji, H., *Macromol. Biosci.*, **2005**, *5*, 569-597.
18. Hughes, J.; Thomas, R.; Byun, Y.; Whiteside, S., *Carbohyd. Polym.*, **2012**, *88*, 165-172.
19. Fukushima, K.; Tabuani, D.; Arena, M.; Gennari, M.; Camino, G., *React. Funct. Polym.*, **2013**, *73*, 540-549.
20. Liu, Y. L.; Shao, J.; Sun, J. R.; Bian, X. C.; Feng, L. D.; Xiang, S.; Sun, B.; Chen, Z. M.; Li, G.; Chen, X. S., *Polym. Degrad. Stabil.*, **2014**, *101*, 10-17.
22. Ray, S. S.; Okamoto, M., *Prog Polym Sci.*, **2003**, *28*, 1539-1641.